

Density Fluctuations in Bisphenol A Polycarbonate and Tetramethyl-Bisphenol A Polycarbonate As Studied by X-ray Diffraction

G. Floudas,* T. Pakula, M. Stamm, and E. W. Fischer

Max-Planck-Institut für Polymerforschung, Postfach 3148, D-6500 Mainz, Germany

Received November 2, 1992; Revised Manuscript Received December 23, 1992

ABSTRACT: Small-angle X-ray scattering (SAXS) is employed to measure the density fluctuations in Bisphenol A polycarbonate (BPA-PC) and tetramethyl-Bisphenol A polycarbonate (TMPC) as a function of temperature (T) in the range 300–510 K. Pressure–volume–temperature (PVT) measurements are made for TMPC in the range 300–539 K and for applied pressures up to 200 MPa. Wide-angle X-ray (WAXS) measurements are performed for both polymers in the range 300–480 K. Using these techniques we characterize the state of order in the two polymers. Whereas from specific volume and WAXS measurements an estimate of the average free volume is obtained, SAXS provides the fluctuations in the free volume. Our results demonstrate that TMPC possesses a higher average free volume and free volume fluctuations as compared to BPA-PC. This result is discussed in terms of the differences in packing and stiffness of chains. By extending this conclusion to other polymers, we suggest that the average free volume and its fluctuations are not the same for different polymers—as it is frequently assumed.

Introduction

Glass formation can be viewed through different approaches.^{1–4} The traditional way to interpret glass formation is through the phenomenological concept of free volume.^{1–3} Albeit there are many successes of the free volume theories in explaining glass formation, it is now recognized that the specific volume (or free volume) alone is not sufficient to characterize the state of order of a glass. Thermal history,⁵ pressure densification,⁶ and suppression of secondary relaxation in some polymer/additive mixtures⁷ are some examples where knowledge of the specific volume of a glassy material is not sufficient to predict its future response. Additional order parameters are necessary for a unique characterization of the glassy state. Alternatively, knowledge of the average free volume together with its fluctuations can explain the observed changes during isothermal annealing, pressure densification, and the suppression of the secondary relaxations. The free volume fluctuations invoked in this picture arise from density fluctuations in the glass which can be evaluated directly with small-angle X-ray scattering (SAXS).

The density fluctuation is defined by

$$\psi(V) = \langle (N - \langle N \rangle)^2 \rangle / \langle N \rangle \quad (1)$$

where N is the number of particles within a reference volume V —of arbitrary shape and size—and $\langle N \rangle$ is the average number of particles. It can be shown that $\psi(V)$ is independent of V as long as the reference volume exceeds values corresponding to distances of atomic correlations.⁸ If a definite size of the reference volume is considered, then the (electron) density fluctuation $\psi_e(V)$ ($\psi_e = Z\psi$, Z is the number of electrons per particle) is given by⁹

$$\psi_e(V) = \int \frac{1}{n} I(Q) \frac{1}{V} [\Phi(Q)]^2 dQ \quad (2)$$

where $\Phi(Q)$ is the Fourier transform of the form factor of the reference volume, n is the average electron density, and $I(Q)$ is the scattered intensity with Q being the magnitude of the scattering vector. In the thermodynamic limit ($V \rightarrow \infty$), $[\Phi(Q)]^2/V$ becomes a delta function and eq

2 gives

$$\lim_{V \rightarrow \infty} \psi_e(V) = \psi_e(\infty) = \lim_{Q \rightarrow 0} \frac{I(Q)}{n} \quad (3)$$

Equation 3 relates the observed density fluctuations with an experimentally obtained quantity: the intensity scattered at $Q \rightarrow 0$.

In a one-component system the particle density fluctuation is related to the isothermal compressibility β_T , by

$$\psi(\infty) = \rho k_B T \beta_T(T) \quad (4)$$

where ρ is the average number density. It is worth mentioning that long-range density fluctuations which give rise to an "excess" intensity have been observed in some supercooled liquids by means of light scattering and are associated with prefreezing phenomena at temperature (T) already above T_g .¹⁰ Such excess intensities have also been observed in some bulk polymers by means of light scattering¹⁰ and SAXS.¹¹ According to eq 4, density fluctuations should have a T dependence similar to that of β_T which is discontinuous at T_g . However, it is only the temperature coefficient of the density fluctuation which is discontinuous at T_g ; the magnitudes of the fluctuations exhibit continuous behavior. In fact, it has been shown that for some polymers eq 4 is valid only at $T > T_g$.¹² In a temperature range below T_g , the density fluctuation can be approximated by¹²

$$\psi(\infty) = \rho k_B T \beta_T(T_g) \quad (5)$$

where $\beta_T(T_g)$ is now the isothermal compressibility at T_g and, at even lower T , $\psi(\infty)$ becomes frozen-in to a constant value. The interpretations for the deviation of the measured density fluctuations by means of SAXS from eq 4, at $T < T_g$, are based on the fact that the glassy state is a nonequilibrium state. One way to account for the excess density fluctuations is to introduce order parameter fluctuations¹² and to assume that below T_g , $\psi(\infty)$ has contributions from dynamic and quasistatic components,¹³ the former (eq 5) due to molecular motions with relaxation times much shorter than the experimental time scale and the latter due to frozen-in fluctuation on glass formation.

The quantity $\psi(\infty)$ can be evaluated experimentally in two ways: either by measuring the isothermal compressibility in a PVT experiment (eq 4) or by direct evaluation from the intensity $I(Q)$ at $Q \rightarrow 0$ from SAXS using eq 3 ($\psi = \psi_0/Z$). Moreover, with the combination of SAXS and WAXS, we can obtain $\psi(\infty)$ and $\psi(V)$, respectively, that is, the long- and short-range density fluctuations as a function of T . The purpose of the present work is to study the density fluctuations in two structurally similar polycarbonates as a function of T both above and below T_g . For this purpose we perform SAXS, WAXS, and PVT measurements with the aim of characterizing the state of order in two similar amorphous polymers. Our results show evidence for reduced long-range ordering and therefore enhanced density fluctuation in the glassy TMPC when compared with BPA-PC. This is discussed in terms of the methyl group substitution in the former which (i) reduces the packing ability in the glassy state and (ii) increases the stiffness of chains, giving a higher T_g .

Experimental Section

Samples. The BPA-PC and TMPC were provided from Bayer AG and had a weight average molecular weight of 2.8×10^4 and 3×10^4 , respectively. The DSC glass transition temperatures were 420 and 471 K, respectively (heating rate 10 K/min). For the X-ray measurements samples of ~ 1 -mm thickness were prepared by heating the polymers above their T_g and by applying pressure with a laboratory press. After the full pressure was applied at the highest temperature, the pressure was released and the sample was cooled to room temperature within ~ 2 h. For the PVT measurements, TMPC was dried for 2 days under vacuum at 473 K and used in the pressure dilatometer in the form of pellets.

SAXS Measurements. The small-angle X-ray scattering measurements were performed with a Kratky Compact camera (A. Paar KG) equipped with a one-dimensional position-sensitive detector (M. Braun). The Ni-filtered Cu K α radiation ($\lambda = 0.154$ nm) was used from a Siemens generator (Kristalloflex 710 H) operating at 35 kV and 30 mA. The sample was kept in the camera under vacuum in a special furnace, and the temperature was maintained by means of a temperature controller. Measurements 1 h long were made in intervals of 10 K within the range 300–510 K, with a stability better than ± 0.2 K. Changes between successive temperatures were completed within ~ 5 min, and a 10-min waiting time was preset for equilibration. The intensity data for Q up to 7 nm^{-1} were collected in a multichannel analyzer and transferred to a Vax station for further analysis. The data were subsequently corrected for absorption, background scattering, and slit-length smearing.¹⁴ Primary beam intensities were determined—in absolute units—by using the moving slit method.

In order to determine the intensity at $Q \rightarrow 0$ we need to fit our raw data over a larger Q range and extrapolate to $Q \rightarrow 0$. For BPA-PC and TMPC we found that the intensity at small Q can be approximated by¹⁵

$$\tilde{I}(Q) = \tilde{I}(0)e^{bQ^2} \quad (6)$$

where $\tilde{I}(Q)$ is the slit-smear intensity and b is a constant. Since $\tilde{I}(0)$ is related to $I(0)$ by a constant factor,⁸ we have evaluated this factor by calibrating the intensity at T above and below T_g . Then the intensity $I(0)$ can be evaluated directly from $\tilde{I}(0)$, making further desmearing of data unnecessary.

Figure 1 shows a plot of the logarithm of the slit-smear intensity $\tilde{I}(Q)$ of BPA-PC at three temperatures: below, near, and above T_g . Within the T range studied, eq 6 was found to describe the data reasonably well, except for the very small Q range which was excluded from the intensity extrapolation to $Q \rightarrow 0$. The discussion on the possible origin of the increase at small Q is beyond the scope of the present study. However, we would like to mention that long-range density fluctuations¹⁰ may account for the upturn of the intensity at small Q . Figure 2

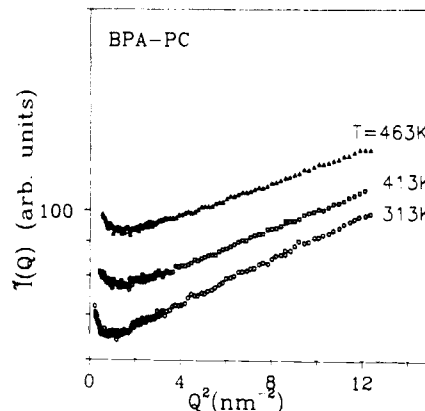


Figure 1. Slit-smear intensities $\tilde{I}(Q)$ for BPA-PC at three temperatures: below (313 K), near (413 K), and above (463 K) T_g . Notice the linearity of the data in the plot $\ln \tilde{I}$ versus Q^2 .

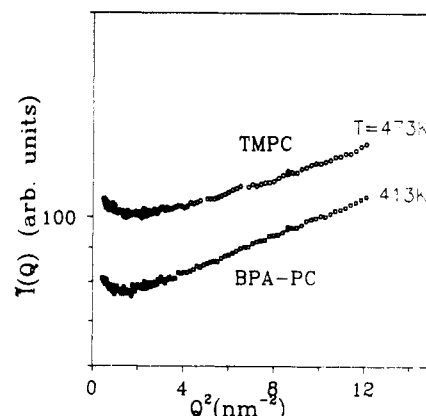


Figure 2. Comparison of the slit-smear intensities $\tilde{I}(Q)$ for BPA-PC and TMPC at temperatures near the corresponding T_g . Notice the higher $\tilde{I}(Q)$ of TMPC.

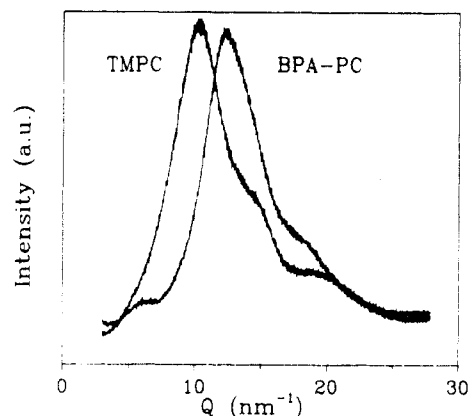


Figure 3. Wide-angle X-ray intensities $I(Q)$ for TMPC and BPA-PC at 300 K.

shows the slit-smear intensity $\tilde{I}(Q)$ of BPA-PC and TMPC for T near their respective T_g 's. The pertinent features of Figures 1 and 2 are discussed in the next section.

WAXS Measurements. The wide-angle X-ray measurements were carried out with a Siemens θ - θ diffractometer (Model D500T) in reflection geometry. Cu K α radiation was used from a Siemens generator (Kristalloflex 710 H) operating at 35 kV and 30 mA and a graphite monochromator was utilized in front of the detector ($\lambda = 0.154$ nm). Measurements were made in the θ range 1 – 20° , with steps of 0.01° , covering the Q range 1.4 – 28 nm^{-1} . The temperature range investigated was 300–480 K. Figure 3 shows the scattered intensity of BPA-PC and TMPC at 300 K.

PVT Measurements. The PVT measurements on TMPC were made isothermally with a pressure dilatometer (constructed by Zoller¹⁶) in the temperature range 300–539 K with a stability of ± 0.2 K and for pressure intervals of 10 MPa up to 200 MPa.

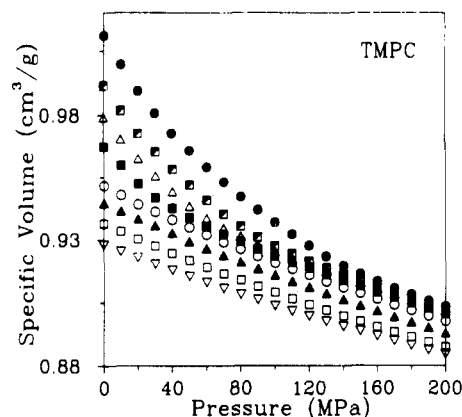


Figure 4. PVT data for TMPC in the form of isotherms: (∇) 300 K; (\square) 358 K; (Δ) 411 K; (\circ) 445 K; (\blacksquare) 479 K; (\triangle) 495 K; (\boxplus) 512 K; (\bullet) 539 K.

Figure 4 shows the specific volume data of TMPC as a function of pressure in the form of isotherms. The isothermal compressibility $\beta_T = -(\partial \ln V / \partial P)_T$ can be obtained from the initial slopes of $\ln V$ versus P as a function of T or evaluated directly from the empirical Tait equation:

$$V(P, T) = V(0, T) \left[1 - 0.0894 \ln \left(1 + \frac{P}{B(T)} \right) \right] \quad (7)$$

which yields $\beta_T(T) = 0.0894B(T)^{-1}$. The parameter $B(T)$ for BPA-PC was obtained from ref 16.

Results and Discussion

The T dependence of the slit-smeared intensities for BPA-PC (Figure 1) as a function of Q plotted versus T displays the main characteristics found in most amorphous polymers investigated by SAXS: The rather small change of the extrapolated intensity $I(0)$ (and therefore of $I(Q)$) in the interval 313–413 K is followed by a stronger temperature dependence in the smaller interval 463–413 K. This observation alone demonstrates the fact that the measured $I(0)$ is not discontinuous at T_g —and therefore eq 4 is not obeyed in the glassy state. This dependence of $I(0)$ on T , which above T_g reflects mainly the change of β_T with T (eq 4) and below T_g contains additional contributions from dynamic and static components, is expected in view of earlier SAXS studies in other amorphous polymers.^{6–9,12,13} In Figure 2, the intensity $I(Q)$ of BPA-PC is compared with that of TMPC for T near their respective T_g . A pertinent feature of Figure 2 is the higher intensity $I(Q)$ for TMPC. The T dependence of $I(0)$ for the two polymers is shown in Figure 5. The slopes of the calculated intensities ($I(0) = n^2 k_B T \beta_T(T)$) using the compressibility data above T_g (equilibrium slopes) are also shown in Figure 5. Evidently, $I(0)$ starts to deviate from the equilibrium intensities at their respective T_g . Therefore, $I(0)$ for TMPC at T_g is ~ 590 electrons²/nm³ and higher than that of BPA-PC (~ 430 electrons²/nm³). It is worth noticing that the ratio $I(0)^{\text{TMPC}}/I(0)^{\text{BPA-PC}}$ at $T = T_g$ resembles the ratio $T_g^{\text{TMPC}}/T_g^{\text{BPA-PC}}$ (~ 1.35). Such behavior for $I(0)$ has not been reported before,^{8,9,12} mainly because polymers studied earlier had quite similar T_g 's (i.e., polystyrene (PS), poly(methyl methacrylate) (PMMA)).

The particle density fluctuation $\psi(\infty)$ measured by SAXS can be evaluated from the $I(0)$ data shown in Figure 5 using eq 3. The resulting $\psi(\infty)$ is shown in Figure 6 for both polymers as a function of T equidistant from their T_g 's. The T dependence of $\psi(\infty)$ mimics that of $I(0)$: a strong dependence at $T > T_g$ is followed by a weak dependence at $T < T_g$, without the discontinuity predicted

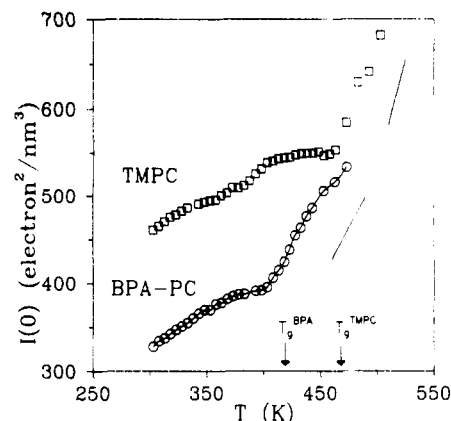


Figure 5. Desmeared intensities $I(0)$ for BPA-PC and TMPC plotted as a function of temperature. Solid lines represent the calculated slopes from the compressibility data using eq 4. Notice that the departure from the equilibrium starts at $T = T_g$.

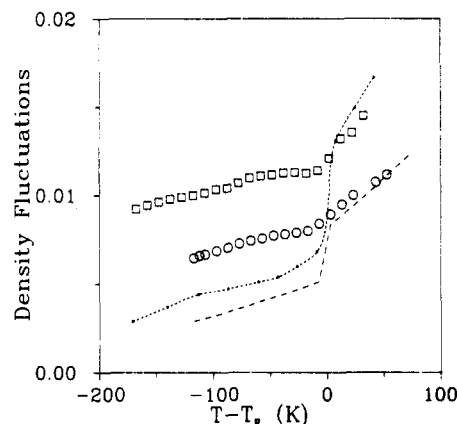


Figure 6. Particle density fluctuations, measured by SAXS, for BPA-PC (\circ) and TMPC (\square) as a function of $T - T_g$. The dotted line is the calculated density fluctuation of TMPC according to eq 4 from our compressibility data which were measured at temperatures indicated by dots. The dashed line represents the calculated density fluctuation of BPA-PC from the compressibility data of ref 16.

by eq 4. The density fluctuation can also be calculated from eq 4 using the measured compressibilities of TMPC and BPA-PC and is also shown in Figure 6 (dashed lines). At $T > T_g$, the agreement between measured and calculated $\psi(\infty)$ values is reasonable, but at $T < T_g$, the former exceeds the latter by nearly a factor of 2. Below T_g , $\psi(\infty)$ can be described by $\rho k_B T \beta_T(T_g)$ —where $\beta_T(T_g)$ is the compressibility obtained from the PVT measurements in a comparable time scale with $I(0)$ —without, however, displaying a leveling-off to a constant value. This is expected to take place at even lower T .^{7,12} It is worth mentioning with respect to Figure 6, that the value of $\psi(\infty)$ at the T_g of BPA-PC is $\sim 8.7 \times 10^{-3}$, whereas the corresponding value for TMPC is $\sim 1.2 \times 10^{-2}$. The same values for PMMA and PS are $1.9 \times 10^{-2,9}$ and $1.7 \times 10^{-2,8,9}$ respectively. Evidently, the structurally similar polycarbonates possess very different density fluctuations below T_g , when studied by SAXS. This can be rationalized if we think of BPA-PC as being a plasticized product (lower T_g value) of TMPC. It is well-known that density fluctuations are suppressed by plasticization⁷ and this is also observed for the density fluctuations in BPA-PC.

In the following we will employ the free volume fluctuation model^{7,17} to describe the average free volume and its fluctuations in BPA-PC and TMPC. According to this model, the free volume is assumed to have a Gaussian distribution characterized by two parameters: (i) the average free volume (V) and (ii) the distribution

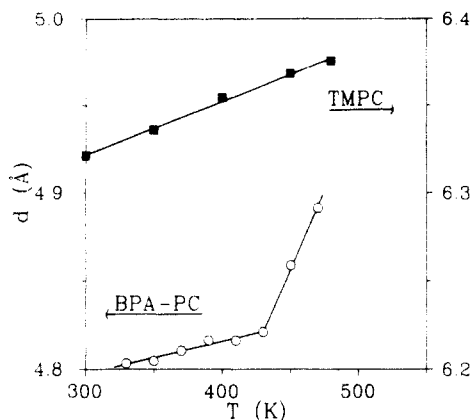


Figure 7. Temperature dependence of the Bragg spacing corresponding to the amorphous peak (Figure 3) of BPA-PC (O) and TMPC (■). Notice the change in slope at the T_g of BPA-PC.

of free volume which is given by the variance $\langle \delta V^2 \rangle^{1/2}$ of the distribution $P(\delta V)$. From the SAXS measurements we have evaluated directly the density fluctuation ψ in both polymers (Figure 6) but in order to make a quantitative picture for the distribution we also need the average free volume $\langle V \rangle$. This can be estimated from the WAXS measurements (Figure 3). The $I(Q)$ curve for BPA-PC (Figure 3) displays two peaks within the measured Q range beyond the "amorphous halo" at 1.3 \AA^{-1} . The peak at $\sim 0.6 \text{ \AA}^{-1}$ has been assigned^{18,19} to intramolecular correlations whereas the position of the amorphous halo reflects largely intermolecular distances and thus the average density (or specific volume) of the material.²⁰ Therefore, the T dependence of the corresponding d spacing ($d = 2\pi/Q_{\text{max}}$), shown in Figure 7, should reflect the change of density with T (thermal expansion). It is worth noticing the change in slope at T_g of BPA-PC which is not observed in TMPC probably because of the higher T_g . In fact the slope below T_g gives—within the experimental error—the thermal expansion of BPA-PC. In comparison, the amorphous halo of TMPC has a peak at $Q = 1 \text{ \AA}^{-1}$ at 300 K, and the difference in the peak position cannot be accounted for by the difference in T_g , since both polymers are glassy at this temperature. The shift of the amorphous peak to lower Q indicates that methyl groups disrupt the ability of chains to pack over a distance of $\sim 5\text{--}6 \text{ \AA}$ and hence produce a higher free volume. This is also indicated by the smaller density of TMPC ($\rho^* = 1.084 \text{ g/cm}^3$) compared to that of BPA-PC ($\rho^* = 1.198 \text{ g/cm}^3$).

With the combined information from SAXS and WAXS we conclude that TMPC possesses a higher free volume and higher free volume fluctuations at $T \leq T_g$. This is illustrated schematically in Figure 8 according to the free volume fluctuation model.^{7,17} The free volume distribution $P(\delta V)$ for TMPC is centered at a higher value of the average free volume $\langle V \rangle$ and it is broader with respect to BPA-PC since $\psi_{\text{TMPC}} > \psi_{\text{BPA-PC}}$ (Figure 6), and this is reflected in the variance of the distribution. The schematic representation of $P(\delta V)$, shown in Figure 8, is valid for $-150 < T - T_g < 0$, since in this range the ratio of the measured density fluctuations for TMPC and BPA-PC remains approximately constant (Figure 6) and is equal to ~ 1.5 .

It is customary to assume that the glass transition is an iso-free volume state²¹ where the free volume is approximately $2.5 \pm 0.5\%$ of the molecular volume.²² Moreover, it is also usually assumed that the free volume distributions are similar in all glassy polymers. However, it has been shown earlier⁷ that free volume fluctuations can be suppressed with the addition of small amounts of a plasticizer and the resulting glasses become more ordered.

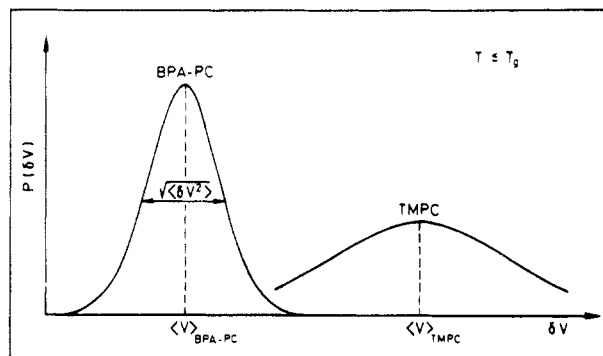


Figure 8. Schematic of the distribution $P(\delta V)$ of the density fluctuations in glassy BPA-PC and TMPC, according to the free volume fluctuation model. Peak positions and widths are determined by the average free volume and its fluctuations, respectively.

Furthermore, voids of different sizes can exist in polymers, albeit the same average free volume exists.²³ The present study provides a more general case. TMPC and BPA-PC possess vastly different (i) average free volumes and (ii) free volume fluctuations.

The diffusion of solvent molecules in glassy polymeric matrices is sensitive to the frozen-in density fluctuations during glass formation. It is expected that the more ordered glasses will produce the higher restriction on the solvent dynamics (solvent modification²⁴). From the two amorphous polycarbonates studied here, we expect solvent diffusion to be less affected by the TMPC matrix as compared to BPA-PC. The recent observation²⁵ of higher transport rates of several gases in glassy TMPC (compared to BPA-PC), is in agreement with our X-ray results.

Conclusions

A unique characterization of the state of order in glassy polymers—without any assumption—requires knowledge of at least two order parameters: (i) the average free volume $\langle V \rangle$ and (ii) its fluctuations $\langle \delta V \rangle$. In the present study, an example is given where $\langle V \rangle$ and $\langle \delta V \rangle$ have been determined to be different for the two polycarbonates studied. This is a result of the methyl substitution which causes a less efficient chain packing in glassy TMPC. In view of our results, the "universality" in values of $\langle V \rangle$ and $\langle \delta V \rangle$ for different polymers must be questioned.

Acknowledgment. G.F. is indebted to Professor R.-J. Roe for helpful discussions. Financial support by the German Science Foundation (Sonderforschungsbereich 262) is highly appreciated.

References and Notes

- (1) Gibbs, J. H.; DiMarzio, E. A. *J. Chem. Phys.* **1958**, *28*, 373.
- (2) Adam, G.; Gibbs, J. H. *J. Chem. Phys.* **1965**, *43*, 139.
- (3) Turnbull, D.; Cohen, M. H. *J. Chem. Phys.* **1961**, *34*, 120.
- (4) Cohen, M. H.; Grest, G. S. *Phys. Rev. B* **1979**, *20*, 1077.
- (5) Götze, W. In *Liquids, Freezing and the Glass Transition*; Hansen, J. P.; Levesque, J. Zinn-Justin, Eds.; North-Holland: Amsterdam, 1991.
- (6) Kovacs, A. J.; Aklonis, J. J.; Hutchinson, J. M.; Ramos, A. R. *J. Polym. Sci., Polym. Phys. Ed.* **1979**, *17*, 1097.
- (7) Curro, J. J.; Roe, R.-J. *J. Polym. Sci., Polym. Phys. Ed.* **1983**, *21*, 1785.
- (8) Fischer, E. W.; Hellmann, G. P.; Spiess, H. W.; Höth, F. J.; Ecarius, U.; Wehrle, M. *Makromol. Chem., Suppl.* **1985**, *12*, 189.
- (9) Roe, R.-J.; Curro, J. J. *Macromolecules* **1983**, *16*, 428.
- (10) Rathje, J.; Ruland, W. *Colloid Polym. Sci.* **1976**, *254*, 358.

- (10) Fischer, E. W.; Becker, Ch.; Hagenah, J.-U.; Meier, G. *Prog. Colloid Polym. Sci.* **1989**, *80*, 198.
- (11) Floudas, G.; Pakula, T.; Fischer, E. W. Manuscript in preparation.
- (12) Wendorff, J. H.; Fischer, E. W. *Kolloid Z. Z. Polym.* **1973**, *251*, 876.
- (13) Roe, R.-J.; Song, H.-H. *Macromolecules* **1985**, *18*, 1603.
- (14) Strobl, G. R. *Acta Crystallogr.* **1970**, *A26*, 367.
- (15) Tanabe, Y.; Müller, N.; Fischer, E. W. *Polym. J.* **1984**, *16*, 445.
- (16) Zoller, P. *J. Polym. Sci., Polym. Phys. Ed.* **1982**, *20*, 1453.
- (17) Bueche, F. J. *Chem. Phys.* **1953**, *21*, 1850.
- (18) Mitchell, G. R.; Windle, A. H. *Colloid Polym. Sci.* **1985**, *263*, 280.
- (19) Schubach, H. R.; Heise, B. *Colloid Polym. Sci.* **1986**, *264*, 335.
- (20) Guinier, A. *X-ray Diffraction*; W. H. Freeman and Co.: New York, 1963.
- (21) Fox, T. G.; Flory, P. J. *J. Appl. Phys.* **1950**, *21*, 58.
- (22) Ferry, J. D. *Viscoelastic Properties of Polymers*; J. Wiley: New York, 1980; Chapter 11 (see also references therein).
- (23) Hinkley, J. A.; Eftekhari, A.; Crook, R. A.; Jensen, B. J.; Singh, J. J. *J. Polym. Sci., Polym. Phys. Ed.* **1992**, *30*, 1195.
- (24) See for example: Morris, R. L.; Amelar, S.; Lodge, T. P. *J. Chem. Phys.* **1988**, *89*, 6523.
- (25) Kim, C. K.; Aguilar-Vega, M.; Paul, D. R. *J. Polym. Sci., Polym. Phys. Ed.* **1992**, *30*, 1131.